Available online at www.sciencedirect.com
SCIENCE DIRECT®
Atmospheric Environment 39 (2005) 1255–1261
ATMOSPHERIC ENVIRONMENT
www.elsevier.com/locate/atmosenv

Validation of a 2D model using observed profiles of SF_6 with main focus on the tropics

Varun Sheel[a,*], Shyam Lal[a], Christoph Brühl[b]

[a]*Space and Atmospheric Science Division, Physical Research Laboratory (PRL), Navrangpura, Ahmedabad 380009, India*
[b]*Max Planck Institut für Chemie (MPIC), 55020 Mainz, Germany*

Received 18 March 2004; accepted 15 October 2004

Abstract

Sulfur hexafluoride (SF_6) is a useful tracer to test the transport behavior of atmospheric models. There have been few measurements of the vertical distribution of SF_6 especially in the tropics, which have restricted the validation of vertical transport in two-dimensional (2D) global models. In an attempt to fill this void, we have used a 2D model in a transient mode to compare the calculated vertical distributions of SF_6 with observations. The gross feature of the simulated vertical profiles compares well with the observations particularly in the tropics. Comparisons with UARS/HALOE CH_4-data show that the sharp vertical gradient above the tropopause and the extremely weak gradient above 25 km in the observations in India are due to the quasi biannual oscillation (QBO). The QBO is not taken into account in the model dynamics but in average between its west and east phase vertical profiles are represented well by the model. We also confirm that global SF_6 source emissions should be distributed on the model grid proportional to electrical power usage.

Keywords: Sulfur hexafluoride; 2D model; Vertical profile; Tropics

1. Introduction

Sulfur hexafluoride (SF_6) is an extremely stable atmospheric trace gas and is produced entirely due to anthropogenic activities. Most of the SF_6 produced worldwide ($\sim 80\%$) comes from electrical equipment like gas-insulated high-voltage circuit breakers, substations, transformers and transmission lines (Niemeyer and Chu, 1992).

Historical release estimates of SF_6 are available, but these are very rough estimates because the amount of gas that is banked inside electrical equipment is highly uncertain. The global increase of SF_6 in the atmosphere provides a reliable accumulation record from which release rates can be calculated. Such an estimate has been provided by Maiss et al. (1996). For an analytical long-term representation of their tropospheric data, they took an emission rate of SF_6 as $E(t) = 0.2(t - 1965.9)$ (Kiloton yr^{-1}).

There is almost no photochemical loss of SF_6 in the troposphere and stratosphere. Its major loss is considered to be the photodissociation by energetic Lyman α radiation in the mesosphere.

The steady increase in the atmospheric concentrations of SF_6 over the past few decades, unaffected by chemical and biological processes, and distinct for both hemispheres is a powerful tool for model investigations of transport processes in the atmosphere. Here we use a two-dimensional (2D) chemical transport model for

*Corresponding author.
E-mail address: varun@prl.ernet.in (V. Sheel).

1352-2310/$ - see front matter © 2004 Published by Elsevier Ltd.
doi:10.1016/j.atmosenv.2004.10.038

such a study. The model has been developed and used for the past 15 years at the Max Planck Institute for Chemistry (MPIC) at Mainz, Germany. We have appropriately modified the MPIC model to include SF_6 in order to study the distribution of the tracer. We call the modified model as PRL-MPIC model and henceforth use this name throughout the text.

2. Model description

The model grid has a horizontal resolution of 10° with 18 latitude points (85°S–85°N) and 34 pressure levels from the ground up to 0.18 hPa (~61 km altitude), with about 2 km spacing in the stratosphere and mesosphere and finer spacing (~0.6 km) in the lower troposphere (up to about 2.5 km).

The chemistry module of the model consists of 73 chemical species, 128 chemical gas-phase reactions, 52 photolysis reactions and the most important heterogeneous reactions on stratospheric sulfate aerosol and polar stratospheric clouds. Short-lived species are grouped in families and solved analytically from the chemical equations. This concept allows an integration time step of 2 h (Gidel et al., 1983; Grooß et al., 1998). Either the flux of a species through the boundary level can be specified or the mixing ratio of the species can be assigned to a fix value.

The photolysis rates are calculated online using a radiative transfer algorithm, based on a modified two-stream method (Zdunkowski et al., 1980). It includes multiple scattering by air molecules, aerosol particles and a climatology for clouds (Brühl and Crutzen, 1988, 1989).

The transport between the model grid boxes is described by the continuity equation. In a 2D model, the large-scale non-zonal fluxes between the model grid points are calculated from mean motions and their variability using an eddy diffusion parameterization (Reed and German, 1965). The diabatic circulation in the stratosphere is calculated in advance (Rosenfield et al., 1987), based on the radiation scheme described by Brühl and Crutzen (1988) and monthly climatological observations of the temperature and ozone. The tropospheric mean winds are taken from observations.

Further details of the model can be found in Gidel et al. (1983) and Brühl and Crutzen (1993) and in the appendix.

3. Simulation of SF_6

We have simulated the transport and concentration of SF_6 for a 20 year period. The model was initialized in 1979 with a globally uniform SF_6 mixing ratio of 0.7327 pptv in the troposphere and 0.366 pptv in the stratosphere. Global SF_6 emission rates have been taken from the estimates of Maiss et al. (1996) based on a linear trend as discussed above. These yearly rates have been listed in Table 1. The simulation for SF_6 was performed with a set of eddy diffusion coefficients, which are purely empirically based, as used in the MPIC 2D model in Ko et al. (1995). The reaction rates of SF_6 with $O(^1D)$ and OH, used in this study are taken from Ravishankara et al. (1993).

Earlier, in the 2D MPIC model, the geographical distribution of emissions of industrial source gases was

Table 1
Global emission rates used in the simulation of SF_6

Year	Kiloton/year	Year	Kiloton/year
1969	0.62	1985	3.82
1970	0.82	1986	4.02
1971	1.02	1987	4.22
1972	1.22	1988	4.42
1973	1.42	1989	4.62
1974	1.62	1990	4.82
1975	1.82	1991	5.02
1976	2.02	1992	5.22
1977	2.22	1993	5.42
1978	2.42	1994	5.62
1979	2.62	1995	5.82
1980	2.82	1996	6.02
1981	3.02	1997	6.22
1982	3.22	1998	6.42
1983	3.42	1999	6.62
1984	3.62		

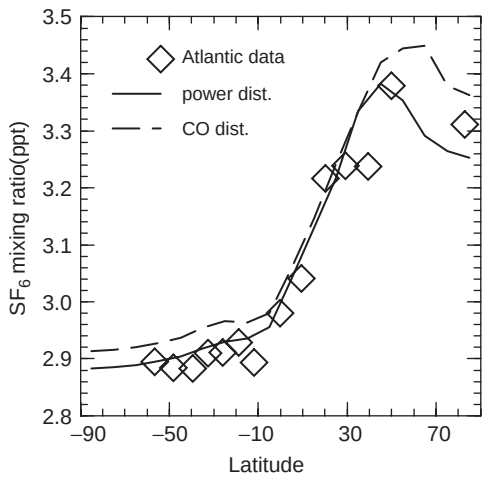

Fig. 1. The mean surface concentration of SF_6 for November 1993 as a function of latitude. The model simulations based on CO distribution (dashed line) and electric power distribution (solid line) are compared with observations from 12 Atlantic transects (triangle) taken from Maiss et al. (1996).

similar to the distribution of carbon monoxide (CO). In the present study we have distributed the global SF_6 emission according to electrical power usage by various countries, since electrical equipment are the major sources. For the other halocarbons, emissions are still distributed according to CO.

As seen in Fig. 1, the model simulation with the latter distribution generated a meridional gradient closer to the observed one than the simulation with SF_6 sources distributed according to CO (Sheel and Lal, 2000).

4. Vertical profiles

Fig. 2 shows the comparison of our model results with the observations. The vertical profile observations have been taken from four balloon flights over Hyderabad, India (17°N) on 26 March 1987, 16 April 1994 and 18 April 1998 (some are published in Patra, 1997; Patra et al., 1997). Also discussed are profiles from Aire sur l'Adour, France (44°N), (30 September 1993) and Kiruna, Sweden (68°N), (20 March 1992 and 18 January 1995), which are published in Harnisch et al. (1996).

The general shape of the vertical profiles (Fig. 2) is that mixing ratio decreases slowly in the troposphere and then decreases faster in the lower stratosphere. This is due to the long lifetime and rapid growth rate of SF_6, which allows it to be used as a tracer for estimation of the mean age of a stratospheric air sample (Patra et al., 1997; Hall and Waugh, 1998). Let us discuss this for Hyderabad (17°N). On 16 April 1994 (see Fig. 2) the observed SF_6 concentration decreases from 3.19 pptv at around 8 km to 3.05 pptv at 17.2 km (near the tropopause). A much faster decrease of 0.06 pptv/km is observed in the lower stratosphere up to about 27 km. The decrease slows down further to about 0.01 pptv/km beyond 27 km. The gradients for 1998 (see Fig. 2) as simulated by the model for Hyderabad are 0.01 pptv/km in the troposphere and 0.08 pptv/km in the lower stratosphere, while the observed gradients are 0.0083 pptv/km in the troposphere and 0.15 pptv/km in the lower stratosphere. The bias between model and observations also seen in 1997 is discussed in the later paragraphs.

A striking feature is seen from the observations. SF_6 concentration decreases very slowly in the troposphere up to about 17 km for Hyderabad and 13 km for Sweden. The decrease is very rapid in the stratosphere up to about 25 km for Hyderabad and 20 km for Sweden and then slows down again above this altitude. In fact the SF_6 concentration above 25 km was almost constant for Hyderabad in 1994. This last feature indicates unusually strong mixing in the region above 25 km and is not reproduced by the model.

The relatively poor agreement in Fig. 2 for 1987 at Hyderabad is due to disturbances by the quasi biannual oscillation (QBO). Measurements on 16 April 1994 represent almost the same QBO phase. The kinks in the SF_6 profiles in the stratosphere correspond to the transition from westerlies to easterlies in the Singapore winds (Marquardt and Naujokat, Free University of Berlin, pers. comm.) at about 24 km and from easterlies to westerlies near 33 km. CH_4 profiles obtained by the Halogen occultation experiment on the Upper Atmosphere Research Satellite (Russell et al., 1993; Park et al., 1996) near 17°N at the same time show a very similar behavior. However, CH_4, in contrast to SF_6, decreases quickly with altitude (Fig. 3) because of chemical sinks in the stratosphere. The region with easterlies promotes vertical mixing, while in the regions with westerlies vertical gradients are built up. The situation is almost similar for the measurements of 1998. In the years 1995 and 1997, which are in the other QBO phase, the vertical transport barriers are vertically shifted, following the zonal wind patterns (Fig. 3). The QBO effect has also been observed in other long-lived tracers like N_2O measured simultaneously during the balloon flights (Patra et al., 2000; Lal and Sheel, 2000)

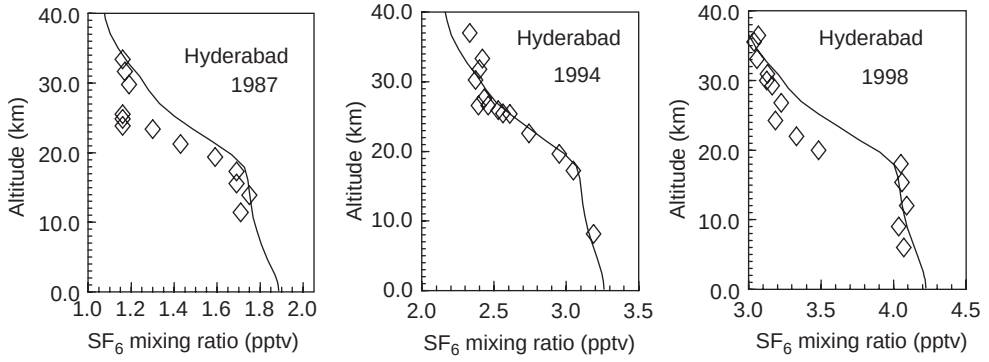

Fig. 2. Vertical distribution of SF_6 obtained from the balloon flight conducted in 1987 (a), 1994 (b) and 1998 (c) from Hyderabad (17°N) (open symbols) compared with the 2D model simulations (solid line).

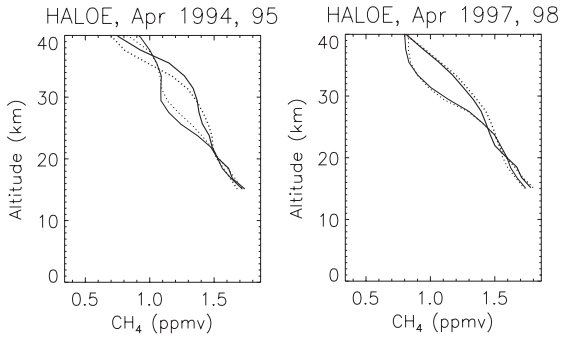

Fig. 3. Profiles of CH_4 obtained by UARS-HALOE for the same dates as in Fig. 2b and c and for the opposite QBO phases (1995, 1997). Solid lines, late April, dotted lines, early April. The thick lines correspond to the years of the SF_6 measurements while thin lines correspond to years 1995 and 1997 (opposite QBO phases).

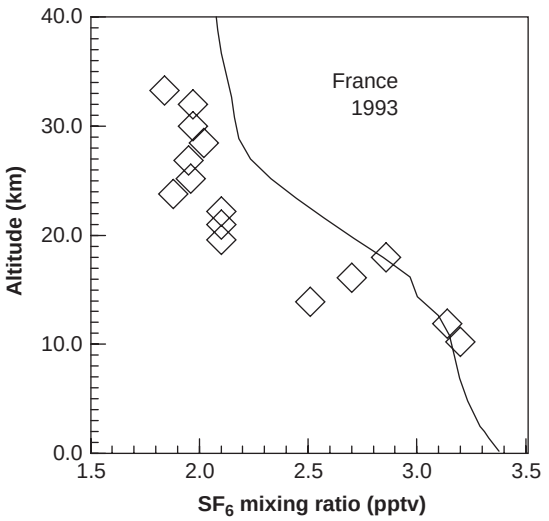

Fig. 4. Vertical distribution of SF_6 measured in 1993 at a midlatitude station in France (44°N) by Harnisch et al. (1996) (open symbols) compared with the 2D model simulations (solid line).

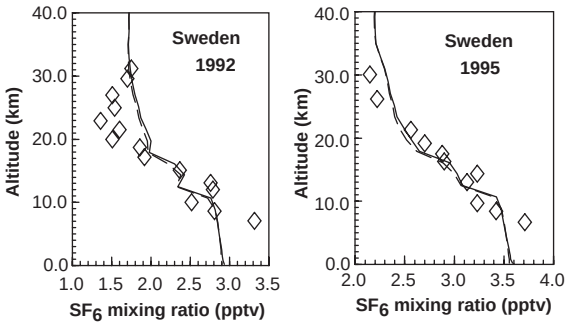

Fig. 5. Vertical distribution of SF_6 measured in 1992 (a) and 1995 (b) at a high-latitude station in Sweden (68°N) by Harnisch et al. (1996) (open symbols) compared with the 2D model simulations for 65°N (solid line) and 75°N (dashed line).

and from observations of trace constituents by HALOE (Dunkerton, 2001). It can also be clearly seen in the vertical propagation of the seasonal signal in tropical stratospheric water vapor (Mote et al., 1996; Niwano and Masato Shiotani, 2001). The profiles calculated by the 2D model represent approximately the average of the two cases of Fig. 3 since the QBO is not included in the model dynamics. However, the model is able to reproduce the increase of SF_6 between 1987 and 1998, indicating that the average upward transport in the tropics to the sink region in the mesosphere is approximately right.

In the midlatitude regions (Fig. 4) the model tends to be high in the lower stratosphere indicating that the subtropical barrier is not strong enough in the model. The model is however in the range of variability with longitude as obtained from HALOE CH_4 data.

In high latitudes (Fig. 5) there is the effect of the polar vortex displaced from the pole containing 'old' air with low SF_6, which cannot be treated in a 2D model. Using the profiles of 75°N as proxi for 'equivalent latitude' relative to the vortex center gives better agreement than using the closest geographical latitude for the observations in the lower stratosphere obviously representing vortex air.

The loss mechanisms of SF_6 in the stratosphere are uncertain (Hall and Waugh, 1998). Vertical profiles have been modeled assuming a loss rate identical to that of CFC-11 in the stratosphere (Ko et al., 1993). However, comparison of vertical profiles of CFC-11 and SF_6 from simultaneous measurements at Hyderabad do not support this result (Patra et al., 1997). We have therefore taken kinetic data for SF_6 from the latest measured estimate as of today by Ravishankara et al. (1993). They report a reaction rate of 1.8×10^{-14} cm^3 mol^{-1} s^{-1} for SF_6 with $O(^1D)$ and an upper limit of 5×10^{-19} cm^3 mol^{-1} s^{-1} for the reaction with OH. This loss process is effective in the mesosphere.

Vertical profiles simulated by the NASA/GSFC 2D model have been earlier compared with 1994 observations over Hyderabad (Patra et al., 1997). The simulation with no photochemical loss of SF_6 shows a better agreement compared to the simulation with SF_6 loss rates assumed identical to CFC-114 and CFC-115. The loss rate coefficients for CFC-114 and CFC-115 by $O(^1D)$ as reported by Ravishankara et al. (1993) are 1.32×10^{-10} and 5.0×10^{-11} cm^3 mol^{-1} s^{-1}, respectively. This justifies the loss rates that we have taken.

The SF_6 vertical profile at 68°N for 1998 also compares well with the profile simulated by Hall and Waugh (1998) using a GCM and assuming no mesospheric loss.

5. Conclusion

In this study we make use of SF_6 measurements, which can provide a valuable constraint on the transport of models, particularly below the middle stratosphere (Hall and Waugh, 1998).

There are differences between model results and observations over Hyderabad in the altitude regions with prevailing westerlies (20–22 km) with the largest differences seen near the transition altitude. In 1994, the vertical extent of easterlies is largest and thus the agreement with model results is better. Comparison with HALOE data of different QBO phases shows that the 2D-model almost simulates the average profiles.

We must emphasize that the vertical comparisons discussed here are with a zonally averaged 2D model. To get better agreement with observation it might help to include a parameterization of QBO effects as in Gray and Pyle (1989). If one has to accurately account for the departures from observations, one must also take into account the longitudinal gradient as discussed in Denning et al. (1999). This would require comparisons with a 3D model.

Acknowledgements

We wish to acknowledge the support of the ISRO-GBP (Bangalore) programme for the balloon experiments in 1994 and 1998. The previous expeditions were conducted under a PRL-MPAE collaborative program. We are grateful to Y.B. Acharya, P. Rajaratnam and members of National Balloon Facility at Hyderabad for their efforts to carry out successful balloon flights. We are thankful to Prabir K. Patra (now at IBM India Research Centre), S. Venkataramani and Duli Chand for analyzing the air samples using gas chromatographic techniques.

We thank J. Harnisch and R. Borchers of Max Planck Institute of Aeronomy (MPAE) for sending us the published vertical profiles for France and Sweden.

Appendix A. Further details of the model

A.1. Chemistry

The chemistry module uses an integration algorithm based on the family concept with a 2 h time step. The chemical families of the 2D model are: odd oxygen (O_x), odd hydrogen (HO_x), reactive chlorine (ClO_x), total inorganic bromine (Br_x), odd nitrogen (NO_y).

A.2. Radiation

The temperatures in the 2D model are based on a climatology by Barnett and Corney (1985) as a function of latitude and pressure for every month of the year.

The cloud cover and distribution are estimated from Warren et al. (1986). The zonal average surface albedo is also taken from climatological data (Robock, 1980). Both cloud cover and surface albedo are given as a function of latitude and season.

The ultraviolet and visible wavelength regions are split into 176 spectral intervals with a higher resolution of 1 nm between 300 and 320 nm (to get the correct photolytical production of $O(^1D)$, which determines OH, HO_2 concentrations)(Madronich and Weller, 1990). In the Schumann–Runge bands of O_2 between 180 and 200 nm the attenuation and absorption of the sunlight is calculated by the parameterization of Allen and Frederick (1982). The calculation of the photolysis rates is performed for a symmetrical diurnal cycle with 2 h time intervals, updated every 15 days of the model integration.

A.3. Transport

The chemical species combined in a family are transported together, similar to the other species whose concentrations only vary slowly. These include H_2O, CH_4, H_2, H_2O_2, N_2O, O_x, HCl, ClO_x, HF, Br_x, CO and the different CFC species. The transport of NO_y species is divided into two groups, HNO3 and the remaining odd nitrogen species (NO_y–HNO_3). Similarly, H_2O_2 is not counted in the HO_x family and is transported separately. Since the lifetime of HO_x is much shorter than the timescales of transport, the HO_x concentrations are calculated from photochemical steady-state assumptions only.

The eddy diffusion coefficients that refer to transport in meridional direction (K_{yy}), vertical direction (K_{zz}) and slanted direction (K_{yz}) are derived empirically for each season. Typical values are $K_{yy} = 5 \times 10^9\,cm^2\,s^{-1}$, $K_{yz} = \pm 5 \times 10^5\,cm^2\,s^{-1}$ and $K_{yy} = 4 \times 10^3\,cm^2\,s^{-1}$ at the 50 hPa pressure level.

The diabatic circulation in the stratosphere is calculated in advance, based on the radiation scheme described by Brühl and Crutzen (1988). The heating rates for this calculation are derived from the infrared absorption calculation of CO_2, O_3, H_2O, CH_4, N_2O and the CFCs by a modified broadband model (Ramanathan, 1976; Kiehl and Ramanathan, 1983) using climatological mixing ratios of these constituents and the radiation scheme described above. From the heating rates, the stream function Ψ is derived by an iterative solution method of the zonally averaged residual Eulerian thermodynamic equation (Solomon et al., 1986) using climatological zonal mean temperatures (Barnett and Corney, 1985). The tropospheric mean winds are taken from observations and the two schemes are connected with stream function and global vertical

mass flux. The wind fields are calculated by differentiating the given stream function Ψ. This method guarantees the conservation of mass, because the continuity equation is fulfilled automatically. The calculated wind fields are updated every month of the model integration.

A.4. Boundary conditions

There are two possibilities for treating transport at the upper and lower boundary of the model. Either the flux of a species through the boundary level can be specified or the mixing ratio of the species can be assigned to a fix value. The first method is better, for e.g., when the emissions on the Earth's surface are well known, while the second method is preferred when observed concentrations at the boundary are available. The model uses a mixture of both methods, but mainly the flux boundary condition (Gidel et al., 1983).

References

Allen, M., Frederick, J.E., 1982. Effective photodissociation cross sections for molecular oxygen and nitric oxide in the Schumann–Runge bands. Journal of Atmospheric Science 39, 2066–2075.

Barnett, J.J., Corney, M., 1985. Middle atmosphere reference model derived from satellite data. In: Labitzke, K., Barnett, J.J., Edwards, B. (Eds.), Handbook for MAP 16. pp. 47–85.

Brühl, Ch., Crutzen, P.J., 1988. Scenarios of possible changes in atmospheric temperatures and ozone concentrations due to man's activities, estimated with a one-dimensional coupled photochemical climate model. Climate Dynamics 2, 173–203.

Brühl, Ch., Crutzen, P.J., 1989. On the disproportionate role of tropospheric ozone as a filter against solar UV-B radiation. Geophysical Research Letters 16, 703–706.

Brühl, Ch., Crutzen, P.J., 1993. MPIC two-dimensional model. In: Prather, M.J., Remsberg, E.E., (Eds.), The Atmospheric Effect of Stratospheric Aircraft, vol. 1292. NASA Ref. Publications, pp. 103–104.

Denning, A.S., Holzer, M., Gurney, K.R., Heimann, M., Law, R.M., Rayner, P.R., Fung, I.Y., Fan, S.-M., Taguchi, S., Friedlingstein, P., Balkanski, Y., Taylor, J., Maiss, M., Levin, L., 1999. Three-dimensional transport and concentration of SF_6: a model intercomparison study (TransCom 2). Tellus 51, 266–297.

Dunkerton, T.J., 2001. Quasi-biennial and subbiennial variations of stratospheric trace constituents derived from HALOE observations. Journal of Atmospheric Science 58, 7–25.

Gidel, L.T., Crutzen, P.J., Fishman, J., 1983. A two-dimensional photochemical model of the atmosphere; 1; chlorocarbons emissions and their effect on stratospheric ozone. Journal of Geophysical Research 88, 6622–6640.

Gray, L.J., Pyle, J.A., 1989. A two-dimensional model of the quasi-biennial oscillation of ozone. Journal of Atmospheric Science 46, 203–220.

Grooß, J.-U., Brühl, C., Peter, T., 1998. Impact of aircraft emissions on tropospheric and stratospheric ozone, part I: chemistry and 2-D model results. Atmospheric Environment 32, 3173–3184.

Hall, T.M., Waugh, D.W., 1998. Influence of nonlocal chemistry on tracer distributions: inferring the mean age of air from SF_6. Journal of Geophysical Research 103, 13,327–13,336.

Harnisch, J., Borchers, R., Fabian, P., Maiss, M., 1996. Tropospheric trends for CF_4 and C_2F_6 since 1982 derived from SF_6 dated stratospheric air. Geophysical Research Letters 23, 1099–1102.

Kiehl, J.T., Ramanathan, V., 1983. CO2 radiative parameterisation used in climate models: comparisons with narrow band models and laboratory data. Journal of Geophysical Research 88, 5191–5202

Ko, M.K.W., et al., 1993. Atmospheric sulfur hexafluoride: sources, sinks and greenhouse warming. Journal of Geophysical Ressearch 98, 10,499–10,507.

Ko, M.K.W., et al., 1995. Model simulations of stratospheric ozone. In: Ennis, C.A., Co. (Ed.), Scientific Assessment of Ozone Depletion: 1994, Global Ozone Research and Monitoring Project—Report No. 37. World Meteorological Organisation, Geneva (Chapter 6).

Lal, S., Sheel, V., 2000. A study of atmospheric photochemical loss of N_2O based on trace gas measurements. Chemosphere: Global Change Science 2, 455–463.

Madronich, S., Weller, G., 1990. Numerical integration errors in calculated tropospheric photodissociation rate coefficients. Journal of Atmospheric Chemistry 10, 289–300.

Maiss, M., Steele, L.P., Francey, R.J., Fraser, P.J., Langenfels, R.L., Trivett, N.B.A., Levin, I., 1996. Sulfur hexafluoride—a powerful new atmospheric tracer. Atmospheric Environment 30, 1621–1629.

Mote, P.W., Rosenlof, K.H., McIntyre, M.E., Carr, E.S., Gille, J.C., Holton, J.R., Kinnersley, J.S., Pumphrey, H.C., Russell III, J.M., Waters, J.W., 1996. An atmospheric tape recorder: the imprint of tropical tropopause temperatures on stratospheric water vapor. Journal of Geophysical Research 101, 3989–4006.

Niemeyer, L., Chu, F.Y., 1992. SF_6 and the atmosphere. IEEE Transactions on Electrical Insulation 27, 184–187.

Niwano, M., Masato Shiotani, 2001. Quasi-biennial oscillation in vertical velocity inferred from trace gas data in the equatorial stratosphere. Journal of Geophysical Research 106, 7281–7290.

Park, J.H., et al., 1996. Validation of halogen occultation experiment CH_4 measurements from the UARS. Journal of Geophysical Research 101, 10,183–10,204.

Patra, P.K., 1997. Study of trace gases in the tropical region. Ph.D. Thesis (Chapter 2), PRL/Gujarat University.

Patra, P.K., Lal, S., Subbaraya, B.H., Jackman, C.H., Rajaratnam, P., 1997. Observed vertical profile of sulphur hexafluoride (SF_6) and its atmospheric applications. Journal of Geophysical Research 102, 8855–8859.

Patra, P.K., Lal, S., Sheel, V., Subbaraya, B.H., Brühl, C., Borchers, R., Fabian, P., 2000. Chlorine partitioning in the stratosphere based on in situ measurements. Tellus 52B, 934–946.

Ramanathan, V., 1976. Radiative transfer with Earth's troposphere & stratosphere: a simplified radiative–

convective model. Journal of Atmospheric Science 33, 1330–1346.

Ravishankara, A.R., Solomon, S., Turnipseed, A.A., Warren, R.F., 1993. Atmospheric lifetimes of long-lived halogenated species. Science 259, 194–199.

Reed, R.J., German, K.E., 1965. A contribution to the problem of stratospheric diffusion by large scale mixing. Monthly Weather Review 93, 313–321.

Robock, A., 1980. The seasonal cycle of snow cover, sea ice and surface albedo. Monthly weather review 108, 267–285.

Rosenfield, J.E., Schoeberl, M.R., Geller, M.A., 1987. A computation of the stratospheric diabatic circulation using an accurate radiative transfer model. Journal of Atmospheric Science 44, 859–876.

Russell, J.M., Gordley, L.L., Park, J.H., Drayson, S.R., Hesketh, W.D., Cicerone, R.J., Tuck, A.F., Frederick, J.E., Harries, J.E., Crutzen, P.J., 1993. The Halogen occultation experiment. Journal of Geophysical Research 98, 10,777–10,797.

Sheel, V., Lal, S., 2000. Long term trends in sulfur hexafluoride. In: Beig, G. (Ed.), Long-term Changes and Trends in the Atmosphere, vol. I. New Age International Publishers, pp. 351–366.

Solomon, S., Kiehl, J.T., Garcia, R.R., Grose, W., 1986. Tracer transport by the diabatic circulation deduced from satellite observations. Journal of Atmospheric Science 43, 1603–1617.

Warren, S.G., Hahn, C.G., London, J., Chervin, R.M., Jenne, R.L., 1986. Global distribution of total cloud cover and cloud type amounts over land. NCAR Technical Note TN-273 + STR, 229pp.

Zdunkowski, W., Welch, R.M., Korb, G., 1980. An investigation of the structure of typical two-stream methods for the calculation of solar fluxes and heating rates in clouds. Contr. Phys. Atmos. 53, 147–166.